B. ROMELCZYK-BAISHYA*[#], D. LUMELSKYJ**, M. STĘPNIEWSKA*, M. GIŻYŃSKI*, Z. PAKIEŁA*

THE MECHANICAL PROPERTIES AT ROOM AND LOW TEMPERATURE OF P110 STEEL CHARACTERISED BY MEANS OF SMALL PUNCH TEST

In this paper small punch test (*SPT*) which is one of miniaturized samples technique, was employed to characterize the mechanical properties of carbon steel P110. The tests were carried out in the range of –175°C to *RT*. Results obtained for *SPT* were compared to those calculated for tensile and Charpy impact test. Based on tensile and *SPT* parameters numerical model was prepared.

8 mm in diameter and 0.8 mm in height (*t*) discs with and without notch were employed in this research. The specimens had different depth notch (*a*) in the range of 0.1 to 0.4 mm.

It was estimated that α factor for comparison of *Tsp* and *DBTT* for carbon steel P110 is 0.55 and the linear relation is $DBTT = 0.55 T_{SPT}$. The numerical model fit with force – deflection curve of SPT. If the factor of notch depth and samples thickness is higher than 0.3 the fracture mode is transformed from ductile to brittle at –150°C.

Keywords: small punch test, carbon steel P110, small samples, low temperature, mechanical properties

1. Introduction

The small punch test (*SPT*) was initially developed in the U.S. and Japan in the 1980s s. Due to running service prolongation program in nuclear industry, research and development of testing techniques with miniaturized specimen were primarily used. Small testing techniques were incentivized due to the high cost of irradiation experiments [1,2].

In present time there is huge demand for a reliable mechanical testing technique which can apply miniature specimens. This open possibility for small punch test which is even considered in practice as non-destructive technique [3]. In this method, usually discs ranging from 3 mm discs to 1×1 cm^2 flat cuboids with a height of less than 1 mm is used [4]. Moreover, sample's preparation doesn't require complicated machining. These advantages caused that *SPT* may be especially useful in example while monitoring the mechanical properties of nanomaterials, coatings or parts under service such as pipes.

Although use of *SPT* has become widespread over the last 30 years with numerous applications which can be found, the standardization of this method still continues to develop [5]. European Committee for Standardization workshop agreement (CWA15627). According to the literature, significant differences between the employed experimental procedures and evaluation techniques still persist. The Small Punch Test is sensitive, not only to precise sensors and loading machines, but also to machining of samples, real geometry of testing jigs and specimens. Moreover for the final results significant influence has a technique of calculating of the parameters. In example yielding force can be estimated as the initial slope shifted by *t*/10, as the initial slope shifted by *t*/100 or the intersection of two tangents in force-deflection curve [6] The difficulties mentioned above are the main reason that SPT results obtained in different laboratories shouldn't be directly compared. Some trends can be found in the literature for results comparison which were obtained from SPT and more standardize technique (Charpy impact or uniaxial tensile test) but the proper indicators should be calculated for each laboratories separately. The most popular correlation between yielding force – yield stress and ultimate force – ultimate tensile stress are in the linear form [6-8]:

$$\sigma_{YS} = \alpha_1 \left(\frac{F_Y}{t^2} \right) + \alpha_2 \tag{1}$$

$$\sigma_{YS} = \alpha_3 \times 2\pi r t F_y - \alpha_4 \tag{2}$$

$$\sigma_{UTS} = \alpha_5 \left(\frac{F_u}{t} \right) + \alpha_6 \tag{3}$$

$$\sigma_m = \alpha_7 \left(\frac{F_u}{t \times u_u} \right) + \alpha_8 \tag{4}$$

*   WARSAW UNIVERSITY OF TECHNOLOGY, FACULTY OF MATERIALS SCIENCE AND ENGINEERING, 141 WOLOSKA STR, 02-507 WARSAW, POLAND
**   INSTITUTE OF FUNDAMENTAL TECHNOLOGICAL RESEARCH, POLISH ACADEMY OF SCIENCES, WARSAW, POLAND

Corresponding auther: barbara.romelczyk.dokt@pw.edu.pl

Similarly a number of equation can be found to compare ductile brittle transit temperature obtained from *SPT* (T_{SPT}) and Charpy impact test (*DBTT*) [9]:

$$DBTT\left(K\right) = \alpha T_{SPT}\left(K\right) + \beta \qquad (5)$$

Another possibility to correlate result is to apply modelling. The numerical modeling, using the finite element analysis (FEA) typically have been used for the in-depth analysis of the *SPT*. Numerical modeling of the *SPT* allows to calibrate material model [10], the study of crack propagation [11] and creep behavior [12] of the material or validate the theoretical predictions [13]. In the present work, the 2D axisymmetric finite element method (FEM) simulation of a small punch test of P110 steel grade has been performed to reproduce the experimental behavior. The following numerical work is aimed at validating the obtained material properties.

Nowadays *SPT* is used to estimate such properties as yield strength and ultimate tensile strength [8], ductile-brittle transition temperature [14], creep strength [15], fracture toughness [16] or fracture characteristic [17]. *SP* tests can either be carried out as creep tests, where a constant force is applied and displacement is measured as a function of time, or as tensile/fracture tests, where a constant displacement rate is applied to the punch and the force is measured as a function of time [5].

2. Methodology

The material was delivered in the form of pipes having an outside diameter of 140 mm and a wall thickness of 10 mm.

Vickers microhardness tests were carried out using a Zwick/Roell ZHU 0.2 hardness tester. Hardness was measured under a load of 1 kg applied for 15 s on the polished samples across the transverse cross-section of pipe. The measurements were performed in accordance to ISO 6507-1:2018. The distance between single measurements was 0.5 mm.

Uniaxial tensile tests were carried out at room temperature using an MTS 810 dynamic testing machine and at –150C using Zwick/Roell250 universal machine. Tensile tests were conducted under the displacement control mode at an initial strain rate of 10^{-3} 1/s. Samples of a 25 mm-gauge section length and 2.5 mm diameter cross-section were used for each tests at RT and –150°C. Specimens were cut off from the longitudinal cross-sections of pipe. Strain was measured using an MTS 634.12F-21 extensometer. Based on the load displacement data, the yield point (YS), ultimate tensile stress (UTS) and elongation to failure (A) were estimated.

The Charpy Impact Test was carried out in accordance with the ISO 26843:2015 standard in a temperature range from –196°C to 25°C using a Zwick/Roell RKP 450 device. For each of the testing temperature one sample of 10×10×55 mm were used.

For the small punch test, a number of samples of 8 mm diameter and 1.2 mm thickness were removed by electrical discharge machining. Samples were cut off along the thickness of the pipe. The samples were then ground to a thickness of (0.800±0.005)

mm using abrasive papers of #120, #400, #600, #800, #1200 and #2400 grit. The grinding was carried out on a Struers LaboPol-21 machine with a rotational speed of 150 rpm. *SPT* experiments were performed on an MTS 858 dynamical testing machine. The tests were performed at a displacement rate of 2 mm/min, while deflection was measured by means of an MTS 634.12F-21 extensometer which had been mounted under the sample. The testing temperature varied between 25°C and –175°C, as measured by a thermocouple located in the testing stand. The samples were mounted between two dies: receiving and clamping which were further immobilized by a screw. The nut was screwed to a sleeve, with 15 Nm torque for the discs. The diameter of the receiving die was 5.4 mm. To minimize friction and to ensure a symmetrical loading of whole sample area, a tubular-shaped puncher with an outer diameter of 3 mm and an inner diameter of 2 mm was employed for loading.

Force-deflection curves were registered during the SPT. The yielding force (F_y) was estimated as the initial slope shifted by $t/10$, where "t" is the initial thickness of the specimen. The ultimate force (F_u) is the maximum force registered during the test. The failure force (F_f) is the force when the drop of load applied is less than 0.8 F_u. U_y, U_u and U_f are corresponding deflections.

Two different methods of calculations were used:
– to the maximum force during the test (E_u) [7],
– to the final fracture of the sample (E_f) [10].

Fractographic observations of the fracture surfaces were then performed using a Hitachi S-3500N scanning electron microscope at an accelerating voltage of 15 kV.

To reproduce the behavior of the material specimen during the small punch test at the room temperature (RT), a FEA has been implemented. Simulation of the SPT has been performed using the ABAQUS explicit dynamic finite element (FE) program [18]. The FE model consists of the specimen, bottom and clamping die, the tubular-shaped puncher. The tools, both dies and puncher have been modeled as a rigid body.

A vertical velocity $v = 0.033$ m/s with a sinusoidal increase and decrease profile has been applied to the puncher. The maximum deflection is $H = 1.5$ mm. The specimen is placed on a die's surface and closed from the top by a blank holder surface. Both surfaces of the tool have been constrained in all directions. The punch deforms the specimen through surface-to-surface contact, which has been used for all interactions taking into account normal and tangential behaviors. The same Coulomb friction $\mu = 0.35$ has been applied to all contacts.

The specimen has been discretized using ABAQUS CAX4R FE. The CAX4R was an 4-node bilinear axisymmetric quadrilateral, reduced integration with hourglass control FE. The mesh was characterized by the same height $h = 20$ μm of the element, and the characteristic size of the mesh is $d = 13.3$ μm under the punch. The Gurson – Tvergaard – Needleman (GTN) constitutive material law has described the material behavior in the simulation. Generally, the GTN models were developed for describing ductile failure by void nucleation and growth in homogeneous metallic materials. Description of the used GTN model with material parameters has been specified in [10]. The

stress-strain curve calibrated to the experimental results has been taken in the following form:

$$\sigma(\varepsilon_p) = K(\varepsilon_0 + \varepsilon_p)^n = 1256(0.026 + \varepsilon_p)^{0.12} \text{ MPa} \qquad (6)$$

The values of material model parameters described in [10] $q_1, q_2, q_3, \varepsilon_n, S_n, f_0, f_n, f_C, f_F$ have been received using the inverse analysis by fitting the numerical force-deflection curve to the experimental. After the fitting procedure, final material parameters have been shown in Tab. 1.

TABLE 1

Material properties of GTN model

q_1	q_2	q_3	ε_n	S_n	f_n	f_C	f_F	f_0
1.2	1	1.44	0.1	0.3	0.0138	0.065	0.12	2e-4

3. Results and discussion

The P110 steel with bainite microstructure was investigated. The required composition by standards for P110 steel is shown in the table 2. The average hardness of the pipe was measured as 309 ±9 HV1.

At room temperature the yield point was estimated as 894 ±12 MPa, the UTS as 952 ±12 MPa, and the elongation to failure as 9.8 ±0.1%. These parameters fulfils expectation of steel pipes used in petroleum and natural gas industries ISO 11960:2011 (Petroleum and natural gas industries – Steel pipes

TABLE 2

Chemical composition

	C	Mn	Ni	Cu	P	S
standards	max. 0,43	max. 1,9	max. 025	max. 0,35	max. 0,03	max. 0,03

for use as casting or tubing for wells) [16]. As it was expected samples deformed at low temperature exhibit higher yield point and ultimate tensile stress. The yield point was estimated as 1 213 ±7 MPa and the UTS as 1 231 ±1 MPa. On the fracture surface necking was observed for samples deformed at both temperature. At RT (Fig. 1c) many dimples were observed, while at –150 °C only the single one was noticed. At low temperature numerous of secondary cracking which propagated perpendicularly to applied force occurred.

In the figure 2 the fracture energy estimated for different temperatures for Charpy impact test is shown.

Based on the absorbed energy drops the *DBTT* was calculated as –45°C (228.15 K). For the damaged samples at upper shelf range from 25 to –35°C (298.15-238.15 K) a rough surface and necking was observed. The samples tested at below –35°C showed a transition from ductile to brittle. Cleavage, plain facets were observed during fractographic investigation. In macroscopic scale no necking occurred.

Results obtained from *SPT* was analysed based on the correlations found in the literature. Yielding force and ultimate force was calculated with proper factor in reference of initial thickness and deflection. The force – temperature curve is shown in the
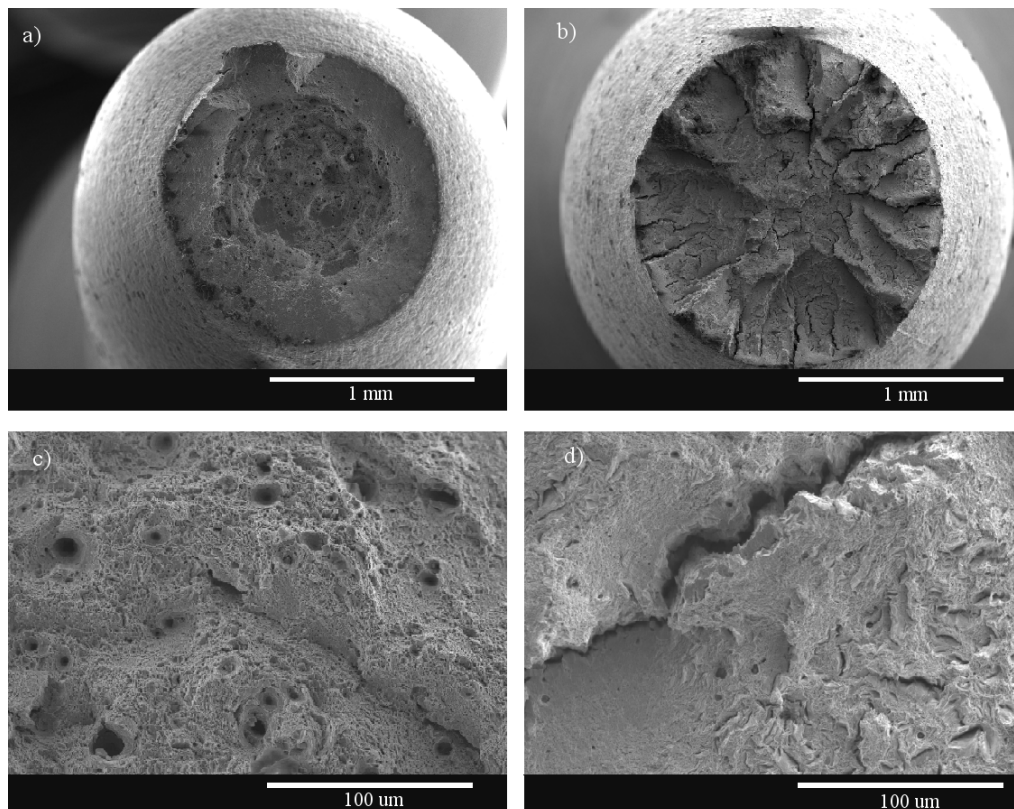

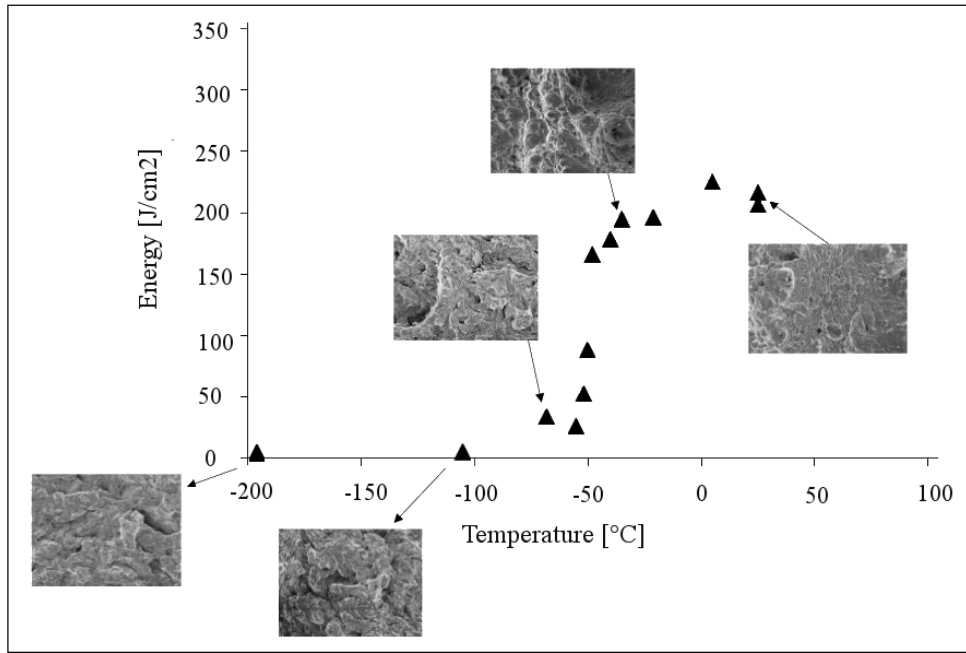Fig. 1. Fracture surface of samples after tensile test at: a), c) *RT* and b), d) –150°C

Fig. 2. The energy and fracture surface obtained for Charpy impact test
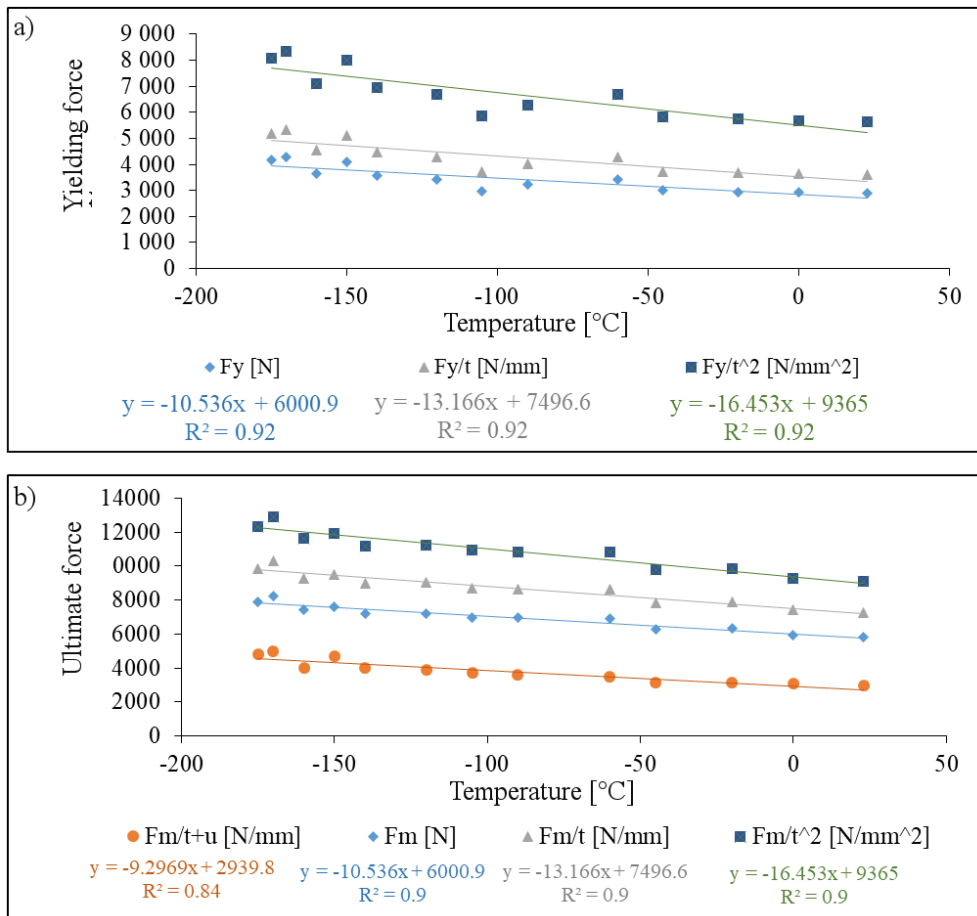

Fig. 3. Yielding (a) and ultimate force (b) obtained for different temperature

figure 3 for both yielding and ultimate force with consideration of different factors.

For all the factors, same trends can be observed – both yielding and ultimate force was increasing with decreasing temperature. These results are comparable with those obtained for standard tensile test.

To estimate transit temperature the fracture energy was calculated. The results are shown in the figure 4.
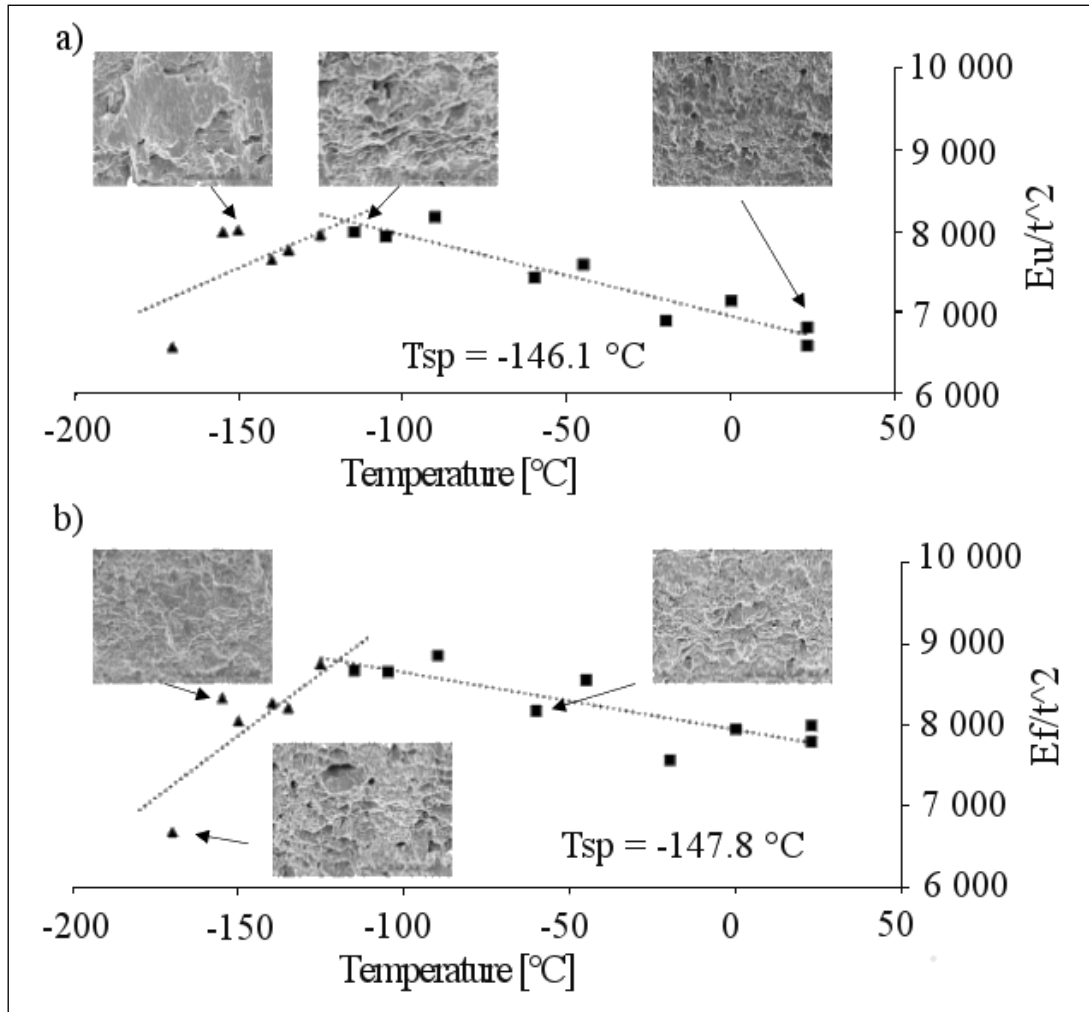
Fig. 4. Temperature dependence of *SPT* fracture energy and thickness: a) energy calculated to ultimate force, b) energy calculated to fracture force

The *Tsp* was calculated as 146.1°C (127.5 K) and −147.8°C (125.35 K). The correlation factor, calculated in Kelvins is 0.55 so the linear relation for P110 steel can be described as follow:

$$DBTT = 0.55T_{SPT}$$

Detailed calculation of *Tsp* and linear correlation was presented in [19]. The difference between *DBTT* and *Tsp* was cause by two factors: size of the samples and velocity of the test. It is typical for small punch test that α is in the range of 0.3-0.5.

While investigating fracture surface it was observed that crack occurs and propagates via a circumferential crack developing outside of the contact area with the punch. At room temperature the fracture mode was ductile, an elongated microstructure elements and microvoids were observed. Near *Tsp* mixed mode occurred, on the fracture surface semi-cleavage areas with decreasing amounts of voids were revealed. At lowest temperature the fracture surface was brittle.

The experimental force-deflection curve of P110 has been compared with the numerical curve obtained for GTN material model with damage (Fig. 5). It might be seen that the FEA results are a slightly higher than the experimental curve. At the failure stage, good coincidence with the experimental curve has been
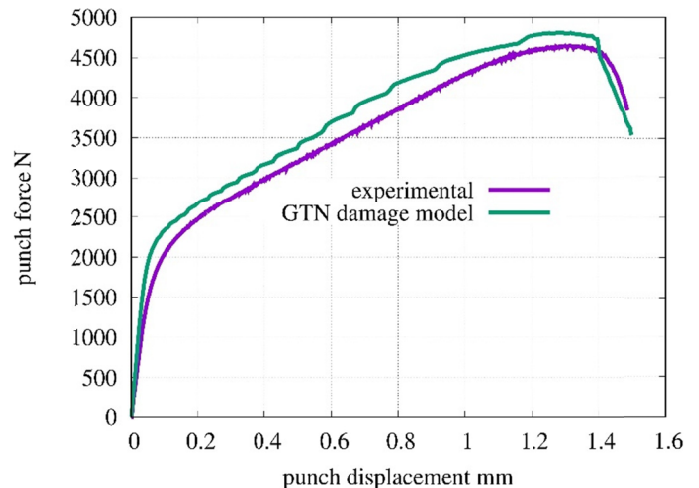

Fig. 5. Comparison between the experimental and numerical force vs. deflection curves of the P110 steel grade *SPT* performed at *RT*

achieved. The discrepancy in overestimation may be caused by simplification of the contact between the holder and specimen. In that case, the overall material response in stiffer in simulation than observed in the experiment.
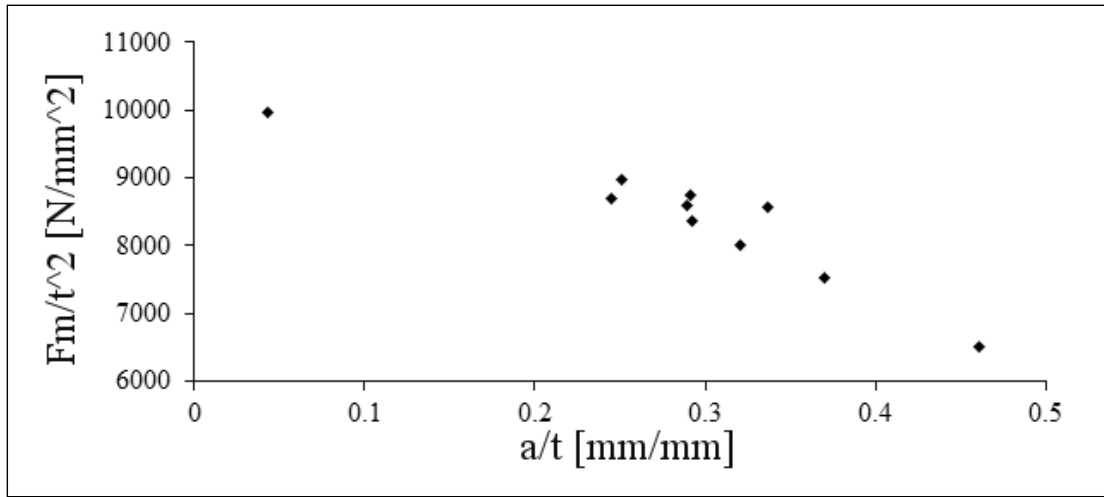
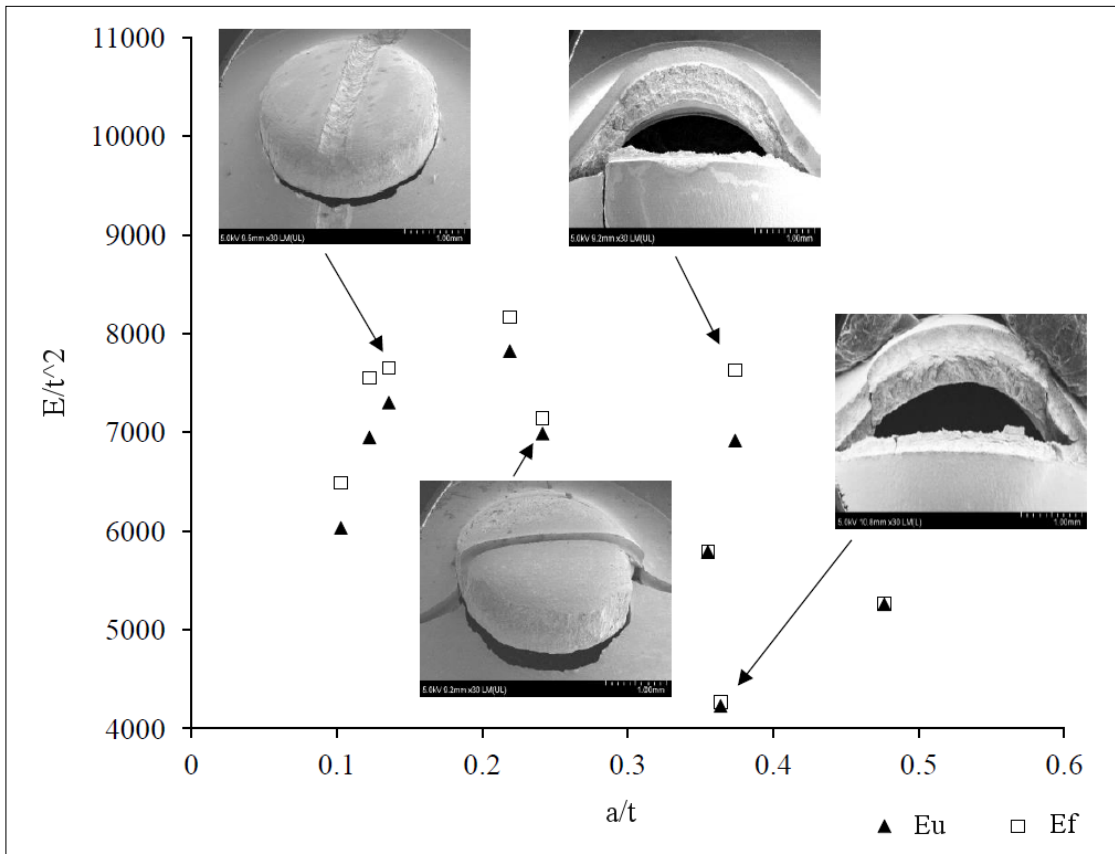Fig. 6. Ultimate force in function of notch depth

Fig. 7. Fracture energy in function of notch depth and exemplary fractured samples

The obtained results show that FEA reproduced the correct behavior of the material during small punch test in all stages of the deformation.

As a next step of investigating P110 steel *SPT* samples with different notch depth were deformed. The ultimate force with dependence of *a/t* parameter is shown in the figure 6 (where a is depth of notch, *t* – initial thickness of the sample). The experiments were carried out at –150°C.

It might have been observed that increasing the notch depth caused the ultimate force decrease. The relation is almost linear.

Notch reduced cross – section of the samples which decrease the strength of material. As it might be seen in figure 7 the notch depth also influence in fracture energy value and crack mode.

Samples with a/t factor lower than 0.3 fractured circumferentially and the influence of notch was negligible in the sense of energy and mode of fracture. Samples with *a/t* factor higher than 0.3 fractured along the notch. In higher resolution observation cleavage fracture was revealed on the surface (Fig. 8).

Fig. 8. Fracture surface of samples with a/t factor higher than 0.3

4. Conclusion

In the paper the mechanical properties of carbon steel P110 was characterised by means of small punch test. The mechanical properties was estimated at room and low temperature. The results was compared with results obtained by standard test as tensile and Charpy impact test. For the research numerical modelling was employed. The material was characterized also in the case of notch influence for *SPT* results at −150°C.

Based on this work, it can be concluded that:

* Similar behaviour of results were observe for *SPT* as for Charpy impact test and uniaxial tensile test. The UTS and Fu increase with temperature decrease. At *RT* fracture surface was ductile while at −150 °C brittle.
* The *Tsp* for P110 steel is in a range of 146.1 °C (127.5K) and −147.8 °C (125.35 K), while the transition temperature estimated from the Charpy impact test is 45°C (228.15 K). The α factor for P110 steel is 0.55 which is caused by smaller size of specimen and test velocity. Near the *Tsp* temperature, the fracture is quasi-brittle.
* The numerical model which was prepared fits with that experimental results of *SPT*.
* at −150°C to obtain brittle fracture while *SPT* critical value of a/t factor (notch depth/initial thickness) is 0.3 for carbon steel P110.

REFERENCES

[1] M.P. Manahan, A.S. Argon, O.K. Harling, J. Nucl. Mater. **104**, 1545-1550 (1981).

[2] M.P. Manahan, Nucl. Technol. **63**, 295-315 (1983).

[3] M.L.Saucedo-Munoz, M.L. Komazaki, T. Takahashi, T. Shoji, J. Mater. Res. **17**, 8, 1945-1953 (2002).

[4] E. Altstadt, H.E. Ge, V. Kuksenko, M. Serrano, M. Houska, M. Lasan, M. Bruchhausen, J. Lapetite, Y. Dai, Y, J. Nucl. Mater. **472**, 186-195 (2016).

[5] European Committee for Standardization, Small Punch Test Method for Metallic Materials, CWA 156272006. (2007).

[6] T.E. García, C. Rodríguez, F.J. Belzunce, C. Suárez, J. Alloys Compd. **582**, 708-717 (2014).

[7] M. A. Contreras, C. Rodriguez, F. J. Belzunce, C. Betegon, Fatigue Fract. Eng. Mater. Struct. **31**, 9, 727-737 (2008).

[8] B. Romelczyk, T. Brynk, R. Molak, A. Jastrzębska, K. Nowak, Z. Pakieła, Key Eng. Mater. **592-593**, 805-808 (2014).

[9] B. Tanguy, J. Besson, R. Piques, A. Pineau, Eng. Fract. Mech. **72**, 1, 49-72 (2005).

[10] S. Nosewicz, B. Romelczyk, D. Lumelskyj, M. Chmielewski, P. Bazarnik, D. Jarząbek, K. Pietrzak, K. Kaszyca, Z. Pakieła, INT J SOLIDS STRUCT, 2018, ISSN 0020-7683, In Press, Accepted Manuscript.

[11] E. Martínez-Pañeda, I.I. Cuesta, I. Peñuelas, A. Díaz, J.M. Alegre, Theor. App. Fract. Mec. **86** part A, 51-60 (2016).

[12] T. Nakata, S.Komazaki, Y. Kohno, H. Tanigawa, Mater. Sci. Eng. A. **666**, 80-87 (2016).

[13] J. Calaf Chica, P. Bravo Díez, M. Preciado Calzada, Mat. Design. **148,** 153-166 (2018).

[14] M.K. Hurst R., Proc. 3th Int. Conf. SSTT, 1-26 (2014).

[15] F. Dobeš, K. Milička, Mater. Charact. **59**, 961-964 (2008).

[16] M. Abendroth, M. Kuna, Eng. Fract. Mech. **73**, 710-725 (2006).

[17] B. Romelczyk-Baishya, K.Łęczycki, M. Płocińska, M. Kulczyk, R. Molak, Z. Pakieła, Arch. Civil Mech. Eng. **18**, 4, 166-1182 (2018).

[18] Abaqus 6.16 Analysis User's Manual SIMULIA, Providence, IR (2016).

[19] M Stępniewska, B Romelczyk-Baishya, T Brynk, M Giżyński, Z. Pakieła, Lecture Notes in Mechanical Engineering, Proceedings of the 7th International Conference on Fracture Fatigue and Wear, Chapter No: 15, 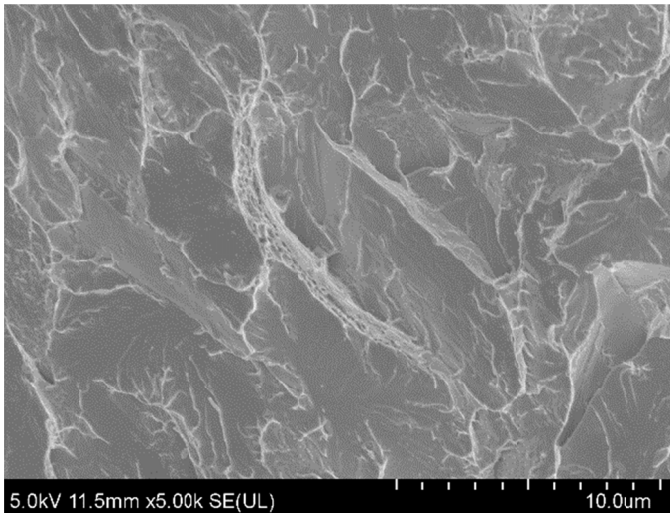151-163 (2018), DOI:10.1007/978-981-13-0411-8_15.